Broad band dielectric relaxation spectroscopy of molecular reorientation in smectic liquid crystalline phases (SmA, SmB, and CrE)

J. Schacht; M. Buivydas; F. Gouda; L. Komitov; B. Stebler; S. T. Lagerwall; P. Zugenmaier; F. Horii

Online publication date: 06 August 2010

PLEASE SCROLL DOWN FOR ARTICLE

Broad band dielectric relaxation spectroscopy of molecular reorientation in smectic liquid crystalline phases (SmA, SmB, and CrE)

J. SCHACHT*, M. BUIVYDAS†, F. GOUDA‡, L. KOMITOV†, B. STEBLER†, S. T. LAGERWALL†, P. ZUGENMAIER§ and F. HORII

Institute for Chemical Research, Kyoto University, Uji, Kyoto 611-0011, Japan
†Department of Microelectronics and Nanoscience,
Chalmers University of Technology, S-412 96 Göteborg, Sweden
‡Physics Department, Faculty of Applied Science, Umm Al-Quara University,
P.O. Box 6427, Makkah, Saudi Arabia
§Institute of Physical Chemistry, Clausthal University of Technology,
Arnold-Sommerfeld-Straße 4, D-38678 Clausthal-Zellerfeld, Germany

Broad band dielectric measurements reveal that the reorientation of non-chiral rod-shaped low molecular mass liquid crystals is active around their molecular long axis and a short axis, in the smectic A and hexatic smectic B phase, respectively, as well as in the soft crystalline E phase of two isomeric stilbene compounds possessing an equal molecular length of their all-*trans*-conformations. One ('generalized') Arrhenius equation describes the temperature dependence of the reorientation around a molecular short axis for each of these phases of both compounds. A change of the activation energy related to the reorientation around a molecular short axis is accompanied by a slowing down of the reorientation around the molecular long axis in the soft crystalline E phase in one of these compounds, compelling evidence for a coupling of both reorientations. This result is discussed with respect to the biaxiality of the soft crystalline E phase.

1. Introduction

A comprehensive description of smectic crystalline phases requires a deep insight into the correlations between their structural and dynamical properties. These correlations provide information about intra- and intermolecular potentials, and play an important role for applications of liquid crystals. In this work our attention is focused on the structure and the molecular dynamics of the orthogonal smectic phases A and B, as well as the orthorhombic soft crystalline E phase, which is closely allied to the smectic phases. The structure of the smectic A phase (SmA) is characterized by a density wave of one-dimensional, quasi-long range positional order with a wave vector parallel to the optical axis (macroscopically uniaxial phase) which coincides with the director describing the average spatial orientation of the molecular long axis (long range orientational order) [1]. Within a particular smectic layer of a hexatic

smectic B phase (SmB), each molecule is surrounded by six nearest neighbours which form a hexagon, at a snap shot. Without creating any quasi-long range positional order within this particular smectic layer, the orientation of these hexagons is macroscopically partially preserved to form quasi-long range bond-orientational order [2–4]. The underlying theoretical concept originates from Landau who recognized that a body of uniform density is not necessarily isotropic [5, 6].

The three-dimensional quasi-long range positional order implies an orthorhombic unit cell to the higher-ordered soft crystalline E (CrE) phase, which might be regarded as a biaxial, strongly distorted 'crystal' [7]. For rod-shaped molecules the molecular long axis points along the long axis of the orthorhombic unit cell and perpendicular to the layer plane. The packing of molecules may be described by a herringbone structure.

Many aspects concerning short and quasi-long range positional order in smectic liquid crystals have been elucidated by wide and small angle X-ray measurements [8–10]. Optical measurements [11], relaxation methods

* Author for correspondence; e-mail: schacht@pc.tu-clausthal.de

[12–14], a variety of NMR experiments [15, 16] and light [17] and neutron scattering [18] provide considerable insight into collective and molecular movement and reorientation, respectively. Substantial work in the field of ^{2}H and ^{13}C nuclear magnetic resonance, as well as ^{14}N nuclear quadrupole resonance [19] has been carried out to elucidate the nature of the internal molecular dynamics as well as the reorientations of molecules around their molecular long and short axes. If these processes are coupled to any reorientation of an electric dipole moment, broad band dielectric spectroscopy [20] provides information concerning the magnitude, the characteristic relaxation time and the activation energy connected to these modes.

In the SmA phase, which exhibits a liquid-like distribution of the mass centres of molecules inside the smectic layers, the reorientation of molecules around their molecular long axis occurs at relaxation frequencies of approximately 100 MHz and it cannot be regarded as free, since it is described by a rotational diffusion process of molecules caused by multiple collisions with their surroundings. However, in the hexatic smectic B phase, due to an increased density and the existence of bond orientational order, this reorientation becomes at least biased or even hindered [21]. In the higher ordered CrE phase this reorientation might be even more hindered or become a librational motion, and a decrease of its relaxation frequency has been found [22].

Tremendous effort has been given to investigations of the reorientation of molecules around a molecular short axis. In the SmA phase of rod-shaped molecules, dielectric measurements exhibit a relaxation frequency of approximately 10 MHz [23, 24], whereas a relaxation frequency of 0.1 MHz is typical for a SmB phase [25–28]. In higher ordered soft crystal phases like CrG [29, 30], a relaxation frequency of 1 to 10 kHz has been established.

It is the purpose of the current paper to investigate the mechanisms related to molecular reorientations in the smectic A and B phases, as well as in the higher-ordered soft crystalline E and in the crystalline phases of two isomeric compounds possessing an equal molecular length. Strong evidence for a coupling of reorientations around the molecular long axis and a short axis is found in the CrE phase of one isomer, as concluded from the temperature dependence of both reorientations.

It should be pointed out that the hexatic smectic B phase (SmB) differs from the higher ordered B phase (CrB), where it has been established that reorientations around a molecular short axis are frozen, whereas reorientations around the molecular long axis are still active [31]. However, both molecular reorientations contribute to the molecular dynamics of the higher ordered E phase.
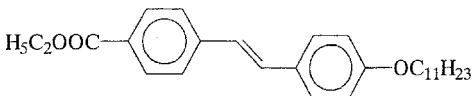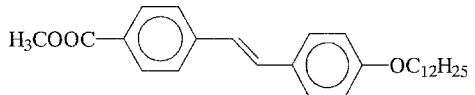
2.   Experimental

The isomeric compounds 4-undecyloxy-4′-carboxyethyl-*trans*-stilbene and 4-dodecyloxy-4′-carboxymethyl-*trans*-stilbene (abbreviated 11Et and 12Me, respectively) possess an almost equal molecular length in their most elongated all-*trans*-conformations. Hence, the aspect ratio of their molecular shape is almost equivalent. Their chemical structures and the sequences of mesomorphic phases are summarized in the table.

Calorimetric studies were carried out with a differential scanning calorimeter (Perkin-Elmer DSC 7) calibrated with an indium standard. A polarizing microscope (Olympus BH-2) equipped with a Mettler FP-52 hot stage and a Mettler FP-5 temperature controlling unit was used for texture analyses. The compounds were examined as films between two untreated glass plates. A Kratky small angle X-ray camera (Anton Paar KG) in association with a one-dimensional positional detector (Firma M. Braun) was employed to study the temperature dependence of the smectic layer spacing. Standard materials were used for calibration.

The dielectric spectra in the low frequency range (5 Hz–13 MHz) were measured by means of a computer controlled set-up using an impedance analyser (Hewlett-Packard, HP 4192A) equipped with a Linkam hot stage and Linkam temperature controlling unit (TMS 600).

Table.   Phase transition temperatures (°C) of the isomeric compounds 11Et and 12Me possessing approximately equal molecular lengths and a similar sequence of enantiotropic orthogonal phases: smectic A (SmA), hexatic smectic B (SmB), and higher-ordered E (CrE). The numbers in parentheses indicate phase transition enthalpies (kJ mol^{-1}). The crystalline phases (Cr) of the two compounds might belong to different space groups.

Phase transition temperatures and enthalpies

11Et

Cr		CrE		SmB		SmA		I
•	108	•	119	•	132	•	144	•
	(42.5)		(2.5)		(5.5)		(9.5)	

12Me

Cr		CrE		SmB		SmA		I
•	132	•	154	•	161	•	166	•
	(44.6)		(3.0)		(5.8)		(12.0)	

An oscillating electric field of amplitude 0.1 MV m^{-1} was used for all measurements, and no bias electric field was applied. Ten measurement points per frequency decade were accumulated, and 64 individual measurements were averaged for a single measurement point at each particular frequency below 10 kHz, and 16 individual measurements at a higher frequency. In the low frequency regime, liquid crystal (LC) cells, built in-house, were used; these consisted of glass plates with an evaporated copper electrode structure. A blocking SiO layer on the copper electrodes prevented any charge injection into the liquid crystal. The active electrode area of these cells was 15 mm^2. A cell thickness of approximately 10 µm was provided by polymer spacers. Each LC cell was calibrated by measurement of the capacitance of the empty cell and its stray capacitance (determined after filling with *n*-hexane) was taken into consideration. Each cell was filled by capillary action near the isotropic to SmA phase transition and the exposure time of the samples to high temperatures was minimized (less than one minute) to keep the static conductivity sufficiently low.

The compounds investigated in this study exhibit an almost planar smectic layer alignment (director **n** parallel to the substrates) within commercial SiO coated LC cells. However, no surfactant was used to achieve a homeotropic smectic layer alignment within the cells; just moderate mechanical shear was applied to generate this texture that differs remarkably from the planar alignment. The copper electrodes did not permit any detailed texture observation in these cells.

The HF reflectometer (Hewlett-Packard HP 4191A) was used for dielectric measurements in the high frequency range (10 MHz–1 GHz). The sample was placed in a capacitor built of two metal plates directly inserted into the reflectometer. A heating system, built in-house, was employed for temperature stabilization. The accuracy of the relative temperature was within 0.1 K (long time stability), and the absolute temperature calibration relative to standard materials was better than ± 1 K for the experimental set-ups described above.

3. Results and discussion

The possible molecular assignments of different absorption peaks will be discussed after an introduction on the general characterization of the different mesophases with emphasis on the texture, DSC and X-ray studies (§3.1). Results obtained in the low frequency regime of the dielectric spectrum will be presented in §3.2, and those from the high frequency dielectric measurements in §3.3.

3.1. *Characterization of mesophases*

A typical fan-shaped texture is observed in the smectic A phase of both compounds. In the smectic B phase,

stripes of slight contrast appear perpendicular to the fans, which makes this phase transition difficult to observe. Nevertheless, a remarkable increase in viscosity indicates a phase transition; this can be noticed from mechanical shearing of the two glass plates. Mechanical shear causes macroscopic flow in the SmA as well as in the SmB phase of these compounds. An abrupt formation of arrays of distinct parallel lines in the texture indicates the SmB to CrE phase transition, and mechanical shear causes no macroscopic flow in CrE but breaks the sample. No supercooling of these phase transitions is observed for a range of cooling rates between 1 and 30 K min^{-1}, whereas the growth of spherulites indicating the crystallization of the CrE phase can be supercooled remarkably.

The phase transitions from isotropic to SmA, to SmB, and to CrE are of first order type. They can be assigned to the peaks of the DSC heating traces for both isomers as shown in figure 1. A shift of a single methylene group from one end of the molecule to the other causes a decrease of the clearing temperature of 22 K, whereas the sequence of mesomorphic phases remains unchanged. The phase transition enthalpies decrease in the following sequence as deduced from the table: crystal/CrE > SmA/isotropic liquid > SmB/SmA > CrE/SmB. Surprisingly, the phase transition from SmA to hexatic SmB has more than half of the transition enthalpy of the SmA to isotropic phase transition, which implies that a considerably large enthalpy is attributed to the formation of the quasi-long range bond-orientational order present in the SmB phase. However, any first order phase transition can be accompanied by a discontinuous change of the density
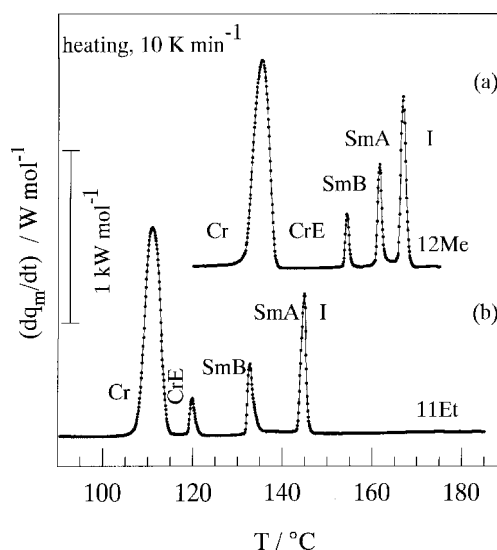

Figure 1. DSC traces for compound 12Me (*a*) and 11Et (*b*): sample mass 5 mg, heating rate 10 K min^{-1}.

of the compound which contributes considerably to the phase transition enthalpy.

A smectic layer distance between 30 and 33 Å characterizes the mesophases (SmA, SmB, and CrE) of both compounds, as can be deduced from the small angle X-ray diffraction patterns depicted in figure 2. The intensity of the second order reflection of the smectic layer is always small in comparison with the first order reflection, and it increases from the SmA to the CrE phase. The temperature dependence of the smectic layer thickness is depicted in figure 3 and increases from 31 Å at the onset of the SmA phase to 32 Å near the SmB phase, probably due to an increase of the nematic order parameter. The smectic layer thickness remains constant at the SmA to SmB phase transition and within the SmB phase. This does not exclude a discontinuous change of the density in the vicinity of the SmA to SmB phase transition. The smectic layer thickness is reduced at the SmB to CrE phase transition in a discontinuous manner and linearly decreases further with decreasing temperature within the CrE phase. Since the nematic order parameter does not decrease with decreasing temperature, the decrease in smectic layer thickness might be explained by an optimized, more dense packing of the molecules in the CrE phase accompanied by a change of the average molecular conformation. A smectic layer distance of 31.0 Å is measured in the CrE phase
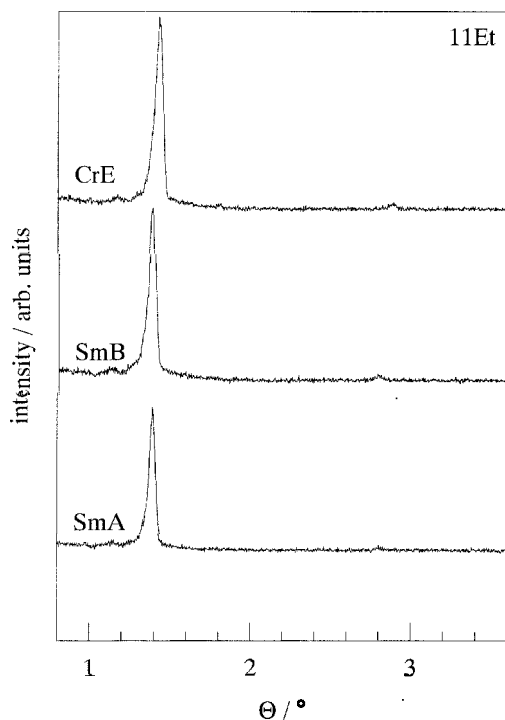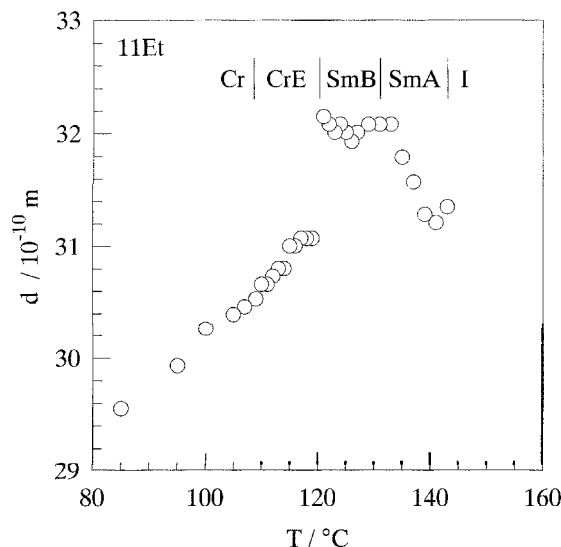

Figure 3.   Temperature T dependence of the smectic layer thickness d of compound 11Et (cooling from the isotropic phase).

near the SmB phase, which is in excellent agreement with the calculated molecular length for their most extended, all-*trans* conformation, and with an internuclear distance of 30.0 Å found for both compounds by molecular simulation (Cerius 2).

3.2. *Dielectric spectroscopy in the low frequency range*
3.2.1. *Compound 12Me*

For compound 12Me, the real part ε' of the complex dielectric permittivity $\varepsilon^* = \varepsilon' - i\varepsilon''$ is plotted as a function of temperature T and frequency f of the electric field in a range between 100 Hz and 5 MHz, figure 4(*a*). In the CrE phase of compound 12Me, a single Debye relaxation is observed and the relaxation frequency shifts to higher frequencies with increasing temperature. A distinct jump of the relaxation frequency by approximately one order of magnitude occurs at the first order CrE to SmB phase transition. In the SmB phase, a single Debye mode is detected, and its relaxation frequency increases with increasing temperature. At the SmB to SmA phase transition, the relaxation frequency increases further by at least one order of magnitude, and reaches the upper limit of the low frequency measurements. For comparison, the corresponding data for the imaginary part ε'' of the complex dielectric permittivity is depicted in figure 4(*b*). The loss of energy due to the single relaxation process is observed most clearly in the CrE phase between 10 and 100 kHz. Also in the SmB phase, maxima related to this process are observed, but these are superimposed by the RC-relaxation of the cell due to a finite resistivity of the electrodes defining the cut-off frequency (~ 50 MHz). The materials have been repeatedly recrystallized from acetone and dimethylformamide to

Figure 2.   Typical X-ray diffraction patterns (CuK_{α}) of 11Et for the CrE, SmB, and SmA phases. A d-spacing of approximately 31 Å characterizes the smectic layer thickness.
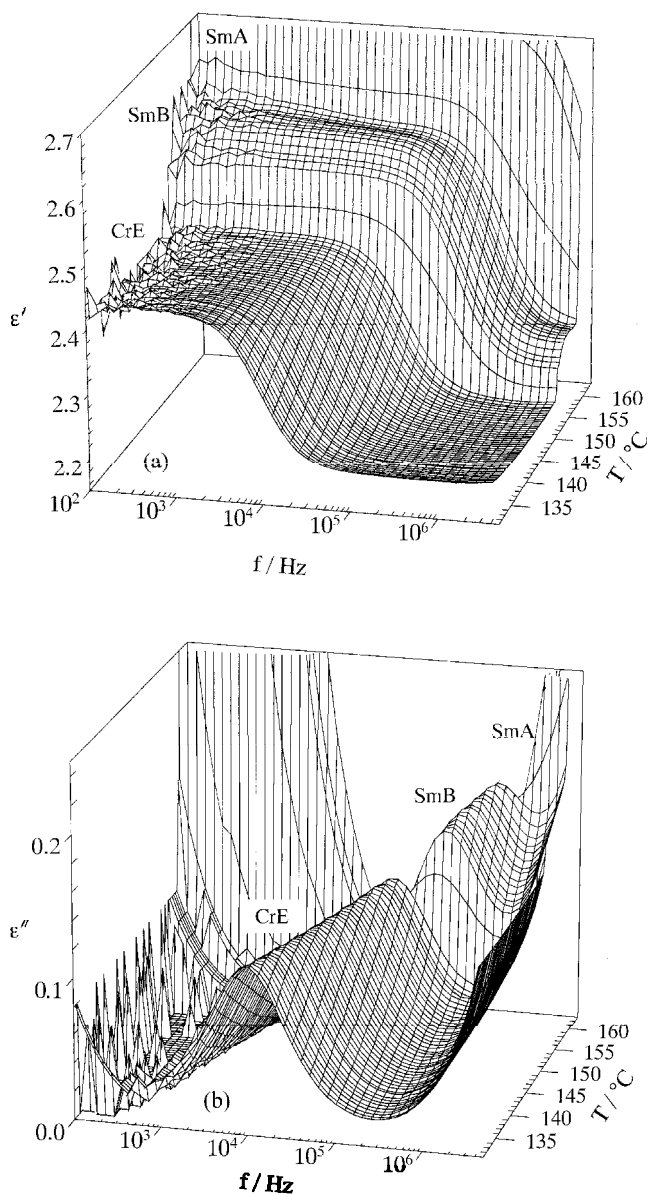
Figure 4. 3D representation of the temperature T and the frequency f (low frequency regime) dependence of the complex dielectric permittivity of compound 12Me (heating from the crystalline phase): (a) real part ε', (b) imaginary part, dielectric loss ε''.

high temperature region of the dielectric spectra, cf. figure 4(b). This does not affect the accuracy of our measurements, since the relaxation frequency of the Debye mode is shifted to higher frequencies with increasing temperature as well.

The dielectric spectra $\varepsilon^*(\omega, T)$ have been subjected to a fitting procedure which takes the following quantities into consideration: the static conductivity σ related to charge carriers, the dielectric increment $\Delta\varepsilon$ and relaxation time τ of a Debye mode assigned to molecular reorientation, the dielectric constant $\varepsilon^{\text{limit}}$ containing all contributions of processes located above the frequency limit of the LCR-bridge, the time τ_{RC} characterizing the RC relaxation of the cell (cut-off), and the vacuum permittivity ε_0

$$\varepsilon^*(\omega, T) = \frac{\sigma}{i\varepsilon_0\,\omega} + \frac{\Delta}{1 + i\omega\,\tau} + \frac{\varepsilon^{\text{limit}}}{1 + i\omega\,\tau_{\text{RC}}}. \qquad (1)$$

Since the Kramers–Kronig relations combine the real and the imaginary part of the complex dielectric permittivity, these two parts are fitted simultaneously to equation (1) and the results are depicted in figures 5(a–c). [A Cole–Cole (or more complicated) equation may be employed to fit the dielectric data, but the resulting distribution parameter is smaller than 0.01, representing a value of no physical meaning. Therefore, this distribution parameter is omitted, and the Cole–Cole formula reduces to Debye's equation (1).] In the CrE and SmB phases the results of the fitting procedure are satisfactory, whereas in the SmA phase of compound 12Me the relaxation frequency reaches the frequency limit of the bridge, and hence only an approximation to the relaxation frequency and the dielectric increment is obtained, and no activation energy is deduced for this mode from the low frequency measurements in this case.

As a result of this fitting procedure, the temperature dependences of the static conductivity σ, the dielectric increment $\Delta\varepsilon$ and the characteristic relaxation time τ of the Debye mode, as well as the dielectric constant $\varepsilon^{\text{limit}}$ up to which the real part of the dielectric permittivity has decreased when reaching the upper frequency limit of the LF bridge, are depicted in figures 6(a–d). The static conductivity approaches a low level of approximately $0.1\,\text{nS m}^{-1}$ in the CrE phase, and increases gradually with increasing temperature until the SmB phase has been reached, figure 6(a). Within the SmB phase, σ remains almost constant, but an increase of approximately two orders of magnitude is found in the vicinity of the SmB to SmA phase transition due to the reduced viscosity and the enhanced mobility of charge carriers. Thermal energy increases the number of charge carriers for temperatures exceeding 170°C and causes σ to increase gradually and irreversibly with

reduce their static conductivity until no further progress could be made. Hence, the contribution of charge carriers to the dielectric loss is sufficiently suppressed, and molecular reorientation with a considerably small dielectric increment (< 1) can be observed down to a frequency limit of 500 Hz. The mobility of charge carriers increases with increasing temperature and above 170°C, thermal heat causes the formation of new charge carriers. Both effects increase the static conductivity related to charge carriers as can be noticed in the low frequency,

increasing temperature. Partial thermal decomposition occurs within the isotropic phase at temperatures above 200°C.

The static conductivity of the crystalline phase is larger than that of the CrE phase. The increase of ε'' at low frequencies in the crystalline phase is assigned to a displacement of charges which might be trapped at grain boundaries in the crystalline state, and causes this behaviour.

The dielectric increment of the Debye mode is independent of temperature in each liquid crystalline phase, as shown in figure 6(*b*), but in the vicinity of the first order phase transitions it increases gradually. Its relaxation time decreases with increasing temperature in each smectic phase and, as expected for a thermally activated process, it obeys an Arrhenius law, cf. figure 6(*c*). In accordance with the behaviour of $\Delta\varepsilon(T)$, the relaxation time $\tau(T)$ decreases discontinuously by approximately one order of magnitude at both first order phase transitions between the smectic phases.

Figure 6(*d*) displays the temperature dependence of $\varepsilon^{\mathrm{limit}}$ which contains all contributions of fast processes compared to the upper frequency limit of the LCR-bridge. $\varepsilon^{\mathrm{limit}}$ is smaller than the dielectric constant measured for the isotropic phase in the vicinity of the SmA phase, which shows the dielectric anisotropy of 12Me to be positive. Due to the increase of the nematic order parameter with decreasing temperature in the SmA phase, $\varepsilon^{\mathrm{limit}}$ decreases in the SmA phase, whereas it remains approximately constant within the SmB, CrE and crystalline phases. Some change of the conformation or packing of molecules, as well as the temperature dependent contribution from the high frequency part of the dielectric spectrum, causes $\varepsilon^{\mathrm{limit}}$ to change at the phase transitions.

3.2.2. *Compound 11Et*

The real part of the complex dielectric permittivity is plotted versus temperature and frequency for compound 11Et in figure 7(*a*). A single Debye mode is found in the SmA, SmB and CrE phases, but in comparison with compound 12Me, this mode is shifted to lower frequencies; hence, its relaxation frequency falls short of 1 kHz in the CrE phase. The contribution of this mode is clearly visible in the SmB and in the SmA phase in contrast to compound 12Me, where this mode was too fast to be determined accurately. Figure 7(*b*) displays the imaginary part of the complex permittivity as a function of
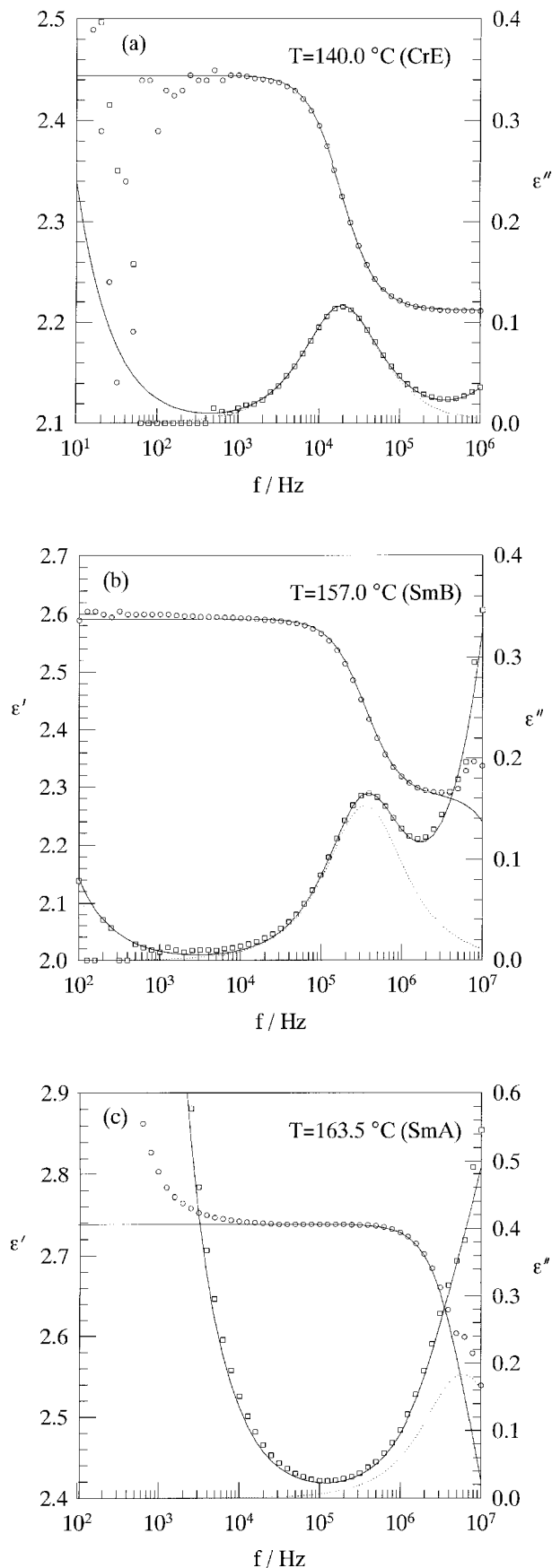

Figure 5. Frequency f dependence of the real part part (ε', ○) and imaginary part (ε'', □) of the complex dielectric permittivity of compound 12Me: (*a*) CrE phase, (*b*) SmB phase, (*c*) SmA phase. The solid lines represent a fit of the experimental data to equation (1).
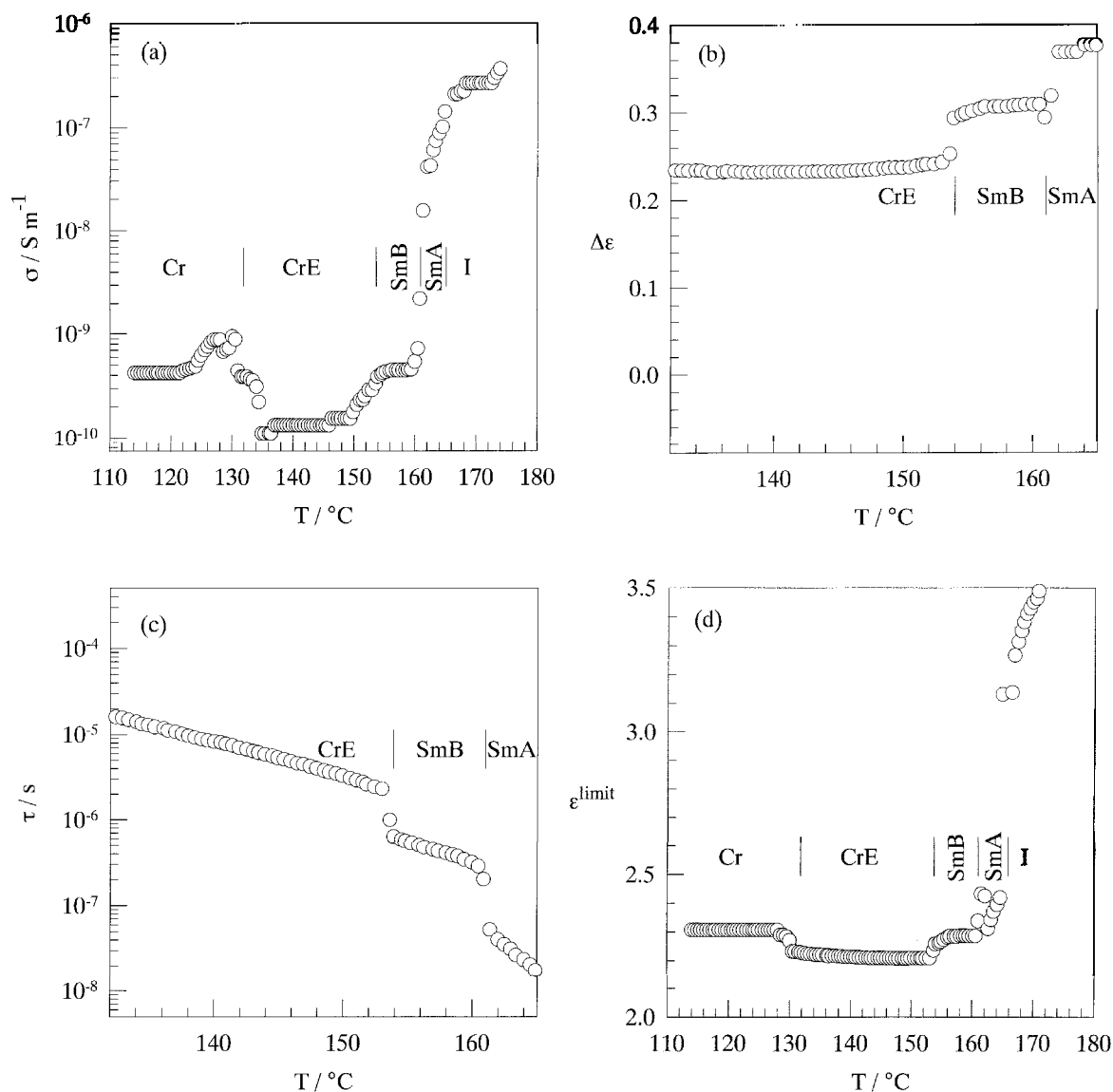
Figure 6. Temperature T dependence of the fitting parameters according to equation (1) (compound 12Me): (a) static conductivity σ caused by charge carriers; (b) dielectric increment $\Delta\varepsilon$ of the Debye mode assigned to a reorientation of molecules around a molecular short axis; (c) relaxation time τ of this Debye relaxation; and (d) the dielectric constant $\varepsilon^{\mathrm{limit}}$ containing all contributions of processes located above the frequency limit of the LCR-bridge.

temperature and frequency; the shift of this mode due to increasing temperature can be noticed, as well as the contribution of the effect of charge carriers and the RC cut-off of the LC cell. The dielectric spectra of compound 11Et are fitted to equation (1) and the results are depicted in figures 8(a–c) for each phase. The best fit is obtained in the SmB phase, but as can be detected in figures 8(a,c) the accuracy of the procedure is still sufficient to evaluate the fitting parameters in the CrE and SmA phases as well. The results of the fitting process are summarized in figures 9(a–d). The temperature dependence of the static conductivity increases gradually with increasing temperature until the SmB to SmA

phase transition is approached. In accordance with the observation made for compound 12Me, σ increases at the SmB to SmA phase transition, as well as at the SmA to isotropic phase transition, due to the decreasing viscosity of the material. Since the clearing point of compound 11Et is lower than for compound 12Me, thermal generation of charge carriers plays a much less important role and plateaus are found in the SmA and isotropic phases. It is worth mentioning that the increase of ε'' at low frequencies in the crystalline phase is much less pronounced than in the case of compound 12Me, and this effect is assigned to the displacement of charge carriers.
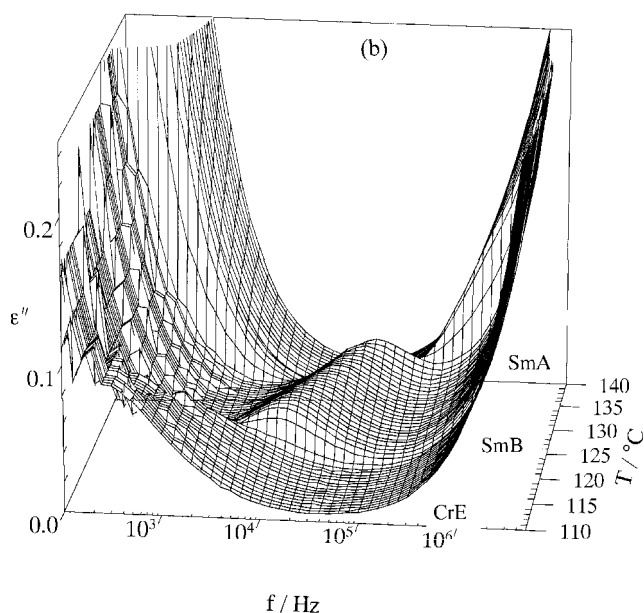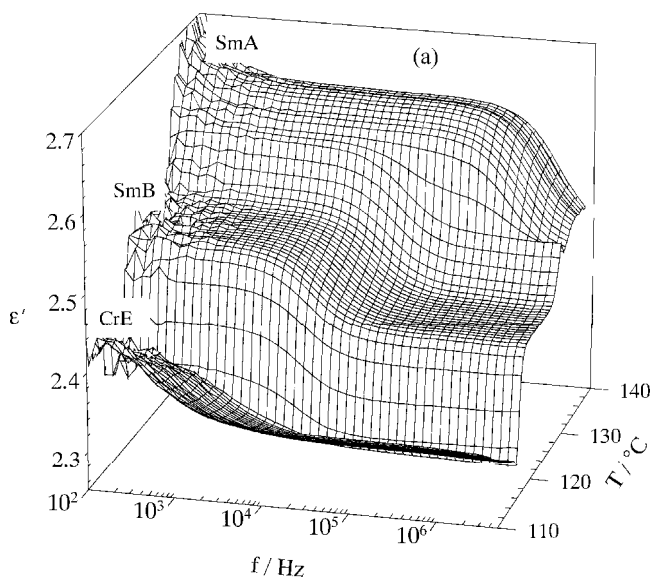
Figure 7. 3D representation of the temperature T and the frequency f (low frequency regime) dependence of the complex dielectric permittivity of compound 11Et (heating from the crystalline phase): (*a*) real part ε', (*b*) imaginary part, dielectric loss ε''.
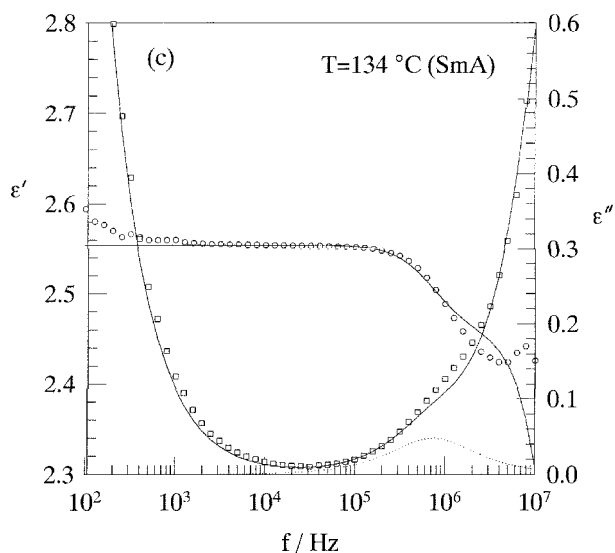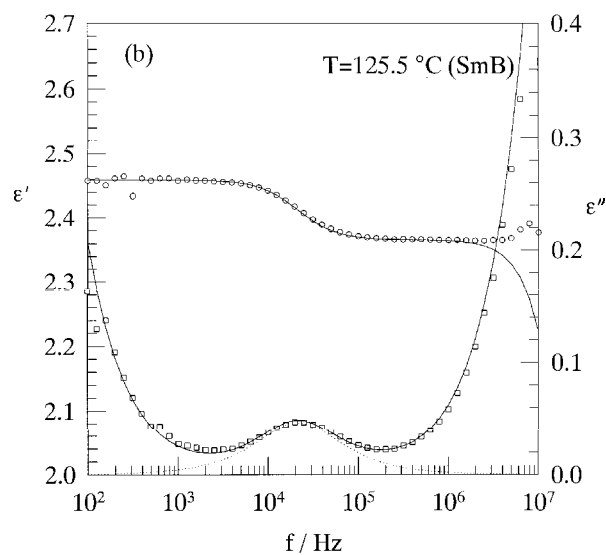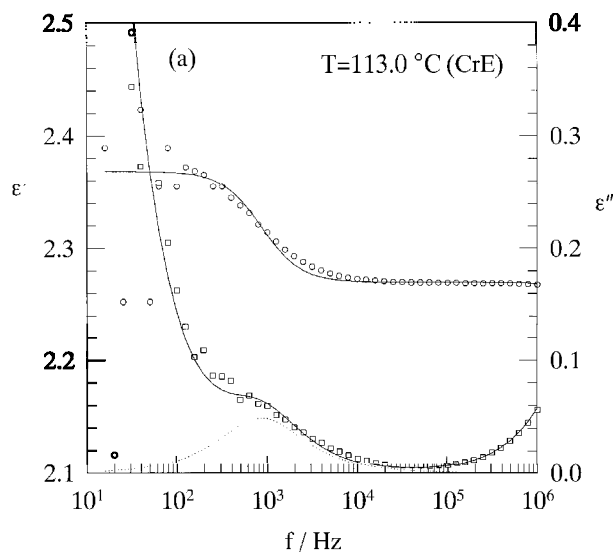
Figure 8. Frequency f dependence of the real (ε', ○) and imaginary part (ε'', □) of the complex dielectric permittivity of compound 11Et: (*a*) CrE phase, (*b*) SmB phase, (*c*) SmA phase. The solid lines represent a fit of the experimental data to equation (1).
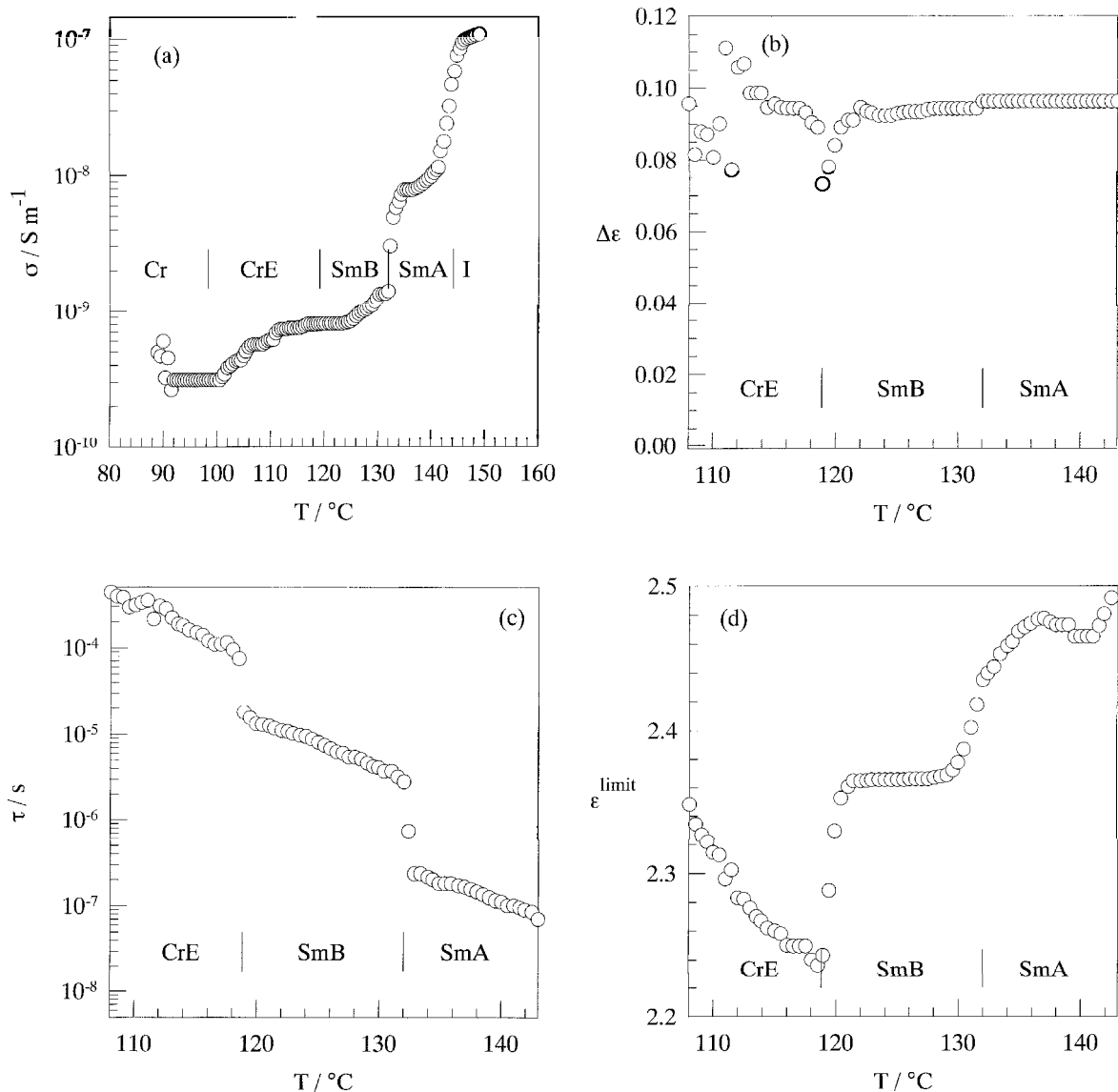
Figure 9. Temperature T dependence of the fitting parameters according to equation (1) (compound 11Et): (*a*) static conductivity σ; (*b*) dielectric increment $\Delta\varepsilon$ of the Debye mode assigned to a reorientation of molecules around a molecular short axis; (*c*) relaxation time τ of this Debye relaxation; and (*d*) the dielectric constant $\varepsilon^{\text{limit}}$ containing all contributions of processes located above the frequency limit of the LCR-bridge.

Figure 9 (*b*) visualizes the temperature dependence of the dielectric increment of the Debye mode; this remains almost constant, but is only one half of the increment for compound 12Me. The temperature dependence of the relaxation time is depicted in figure 9 (*c*) and qualitatively resembles the behaviour of compound 12Me, but the relaxation frequency obtained in the SmB phase of 11Et is as large as the relaxation found at higher temperatures in the CrE phase of its isomer 12Me.

The temperature dependence of $\varepsilon^{\text{limit}}$ is depicted in figure 9 (*d*). In the CrE phase of 11Et, $\varepsilon^{\text{limit}}$ decreases continuously in contrast to the observation made for compound 12Me; this underlines the difference between

the low temperature crystalline phases of the two compounds. Fast processes located above the frequency limit of the low temperature measurements contribute to $\varepsilon^{\text{limit}}$.

3.2.3. *The 'generalized' Arrhenius equation*

The relaxation frequencies of the Debye mode are compared for compounds 11Et and 12Me in figure 10, from which activation energies are determined. In the low frequency range, this Debye mode is usually assigned to reorientations of the molecules around a molecular short axis and is characterized by an activation energy between 71 and $78 \, \text{kJ} \, \text{mol}^{-1}$ generally found for SmA, SmB and CrE phases. Although compounds 11Et and
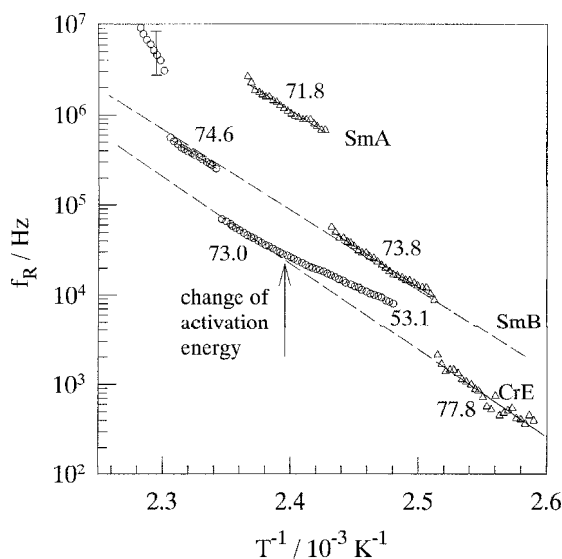
Figure 10.   Logarithmic plot of the relaxation frequency f_R of the Debye mode assigned to a reorientation around a molecular short axis versus the reciprocal temperature $1/T$ for compounds 11Et ($\triangle$) and 12Me ($\bigcirc$). The numbers in the plot represent the activation energies $E_A/\mathrm{kJ\,mol}^{-1}$; no E_A value is reported for the SmA phase of compound 12Me where this mode reaches the upper limit of the LCR-bridge (see error bar). The dashed lines visualize the validity of a 'generalized' Arrhenius equation within the SmB and CrE phases of these compounds.

12Me are isomers with an approximately equal aspect ratio of the molecular shapes of their most elongated all-*trans*-conformations, the relaxation frequency in the CrE phase of 12Me covers the range of frequencies measured in the SmB phase of 11Et. Therefore, reorientations around a molecular short axis in the SmA, SmB and CrE phases are not free, but cooperative reorientations that depend significantly on molecular packing and the structure of the mesophase.

As indicated by the dashed lines in figure 10, a 'generalized' Arrhenius equation describes the temperature dependence of the reorientation around the molecular short axis within the SmB phase of both compounds. By analogy, this holds for the CrE phase of compound 11Et and the high temperature range of the CrE phase of compound 12Me as well, although the temperature dependence of the reorientation around the molecular short axis in the CrE phase of compound 12Me cannot be fitted to an Arrhenius equation over the whole temperature range. Likewise, such a dashed line might also exist for the SmA phases, but the accuracy of the determination of the relaxation frequency in the SmA phase of compound 12Me is not sufficient to draw this conclusion, see figure 5(*c*). Consequently, the assignment of each particular smectic phase is correct, and the same mechanism is responsible for the reorientation

around a molecular short axis in these phases. The pronounced differences between the two compounds are mainly attributed to the lower clearing point of compound 11Et. However, this effect is described well by a generalized Arrhenius equation, which holds for the temperature dependence of the relaxation frequency for both compounds, at least in the SmB and CrE phase (dashed lines in figure 10). Although the activation energy is assumed to decrease from the SmA to the CrE phase, we find an almost equal activation energy. The CrE phase of compound 12Me is an interesting exception.

3.2.4. *Temperature dependence of the activation energy*

Reorientations around the molecular short axis could not be fitted to an Arrhenius equation for the CrE phase of compound 12Me since the slope of $\ln f_R$ versus the reciprocal temperature changes at $\approx 140^\circ\mathrm{C}$, as can be seen from figure 10. Above this temperature an activation energy E_A of $73\,\mathrm{kJ\,mol}^{-1}$ is determined, agreeing with the other activation energies in this study, but below this limit E_A is reduced to $53.1\,\mathrm{kJ\,mol}^{-1}$. The change in activation energy can be best visualized by taking the derivative of $\ln f_R$ with respect to T^{-1} numerically (figure 11); this is possible because of the high accuracy of the measurements (cf. figures 4 and 5). A jump is clearly visible at $138^\circ\mathrm{C}$ and manifests a modification of the mechanism related to the reorientation of molecules around a molecular short axis in the CrE phase, since no phase transition could be detected between 135 and $145^\circ\mathrm{C}$. As may be deduced from figure 12, a slight change of axis for reorientation may serve to provide an explanation since *a* and *b* are not equivalent in the
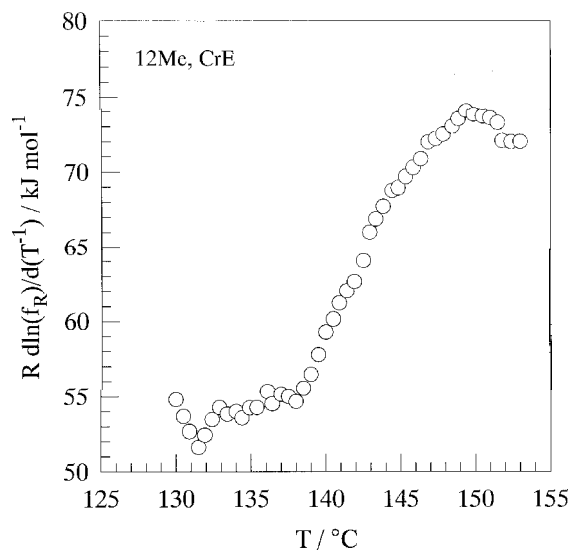

Figure 11.   Temperature T dependence of the logarithmic relaxation frequency inverse temperature gradient $R\,\mathrm{d}\ln f_R/\mathrm{d}(T^{-1})$ (with R the gas constant) for compound 12Me in the CrE phase.
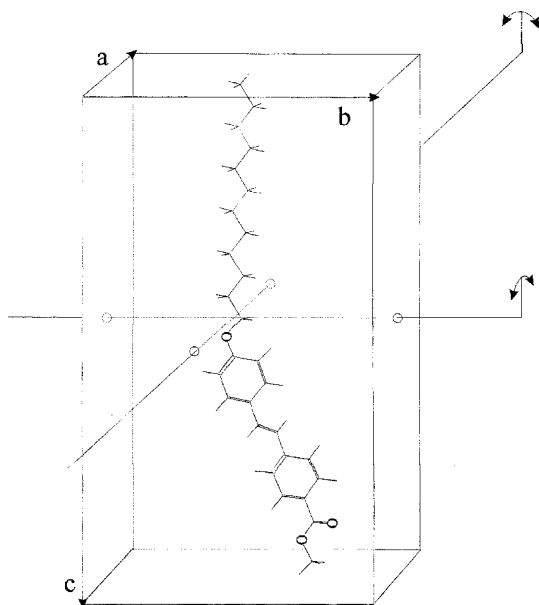
Figure 12. Representation of the two principal short axes around which a molecule can reorient in the biaxial CrE phase.

CrE phase. This change is also expected to affect the reorientation around the molecular long axis slightly, as can be detected by dielectric measurements in the high frequency regime.

3.3. *Dielectric spectroscopy in the high frequency range*

The dielectric spectra in the high frequency range (10 MHz to 1 GHz) are analysed in terms of a Cole–Cole relaxation

$$\varepsilon^{*}_{HF}(\omega, T) = \frac{\Delta\varepsilon}{1 + (i\omega\tau)^{1-\alpha}} \qquad (2)$$

described by its dielectric increment $\Delta\varepsilon$, its relaxation time τ, and the symmetric distribution parameter α. This mode is attributed to the reorientation of molecules around their molecular long axis. A reorientation of the molecular long axis around the director **n**, as well as some intramolecular reorientations of polar functional groups equivalent to conformational changes of the molecules, may affect the dielectric spectra in this frequency range and cause a broadening of this mode described by α. The dielectric measurements in the high frequency regime were performed on cooling, in contrast to the measurements in the low frequency regime.

3.3.1. *Compound 12Me*

For compound 12Me the temperature dependence of the dielectric increment and the relaxation frequency f_R describing the reorientation around the molecular long axis are depicted in figure 13 (*a*). As is commonly found
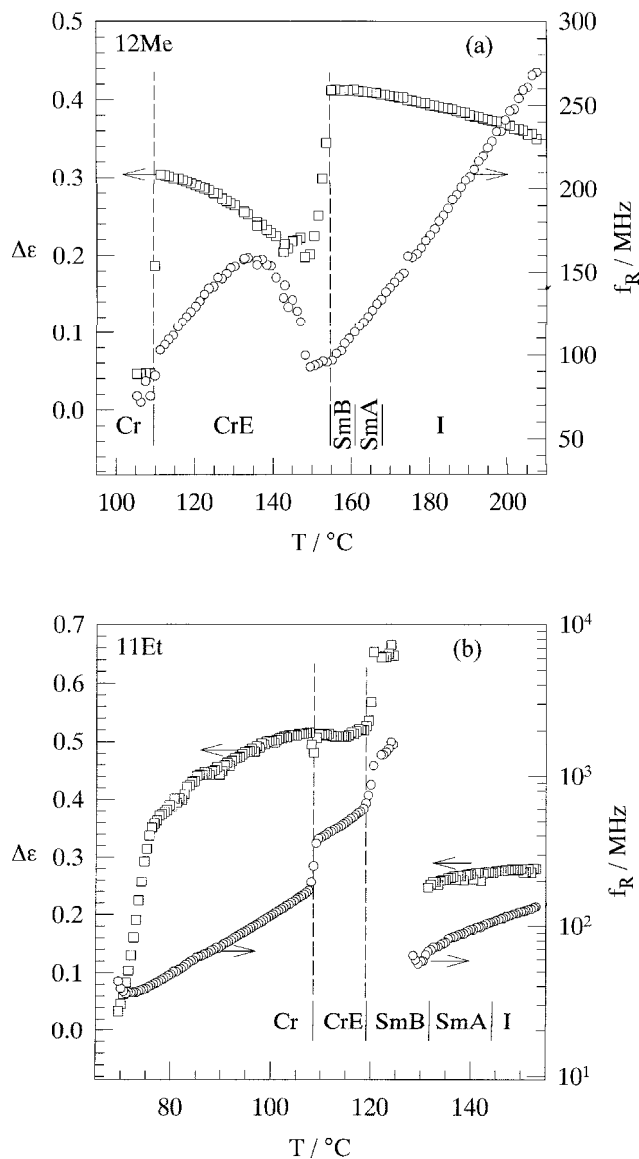

Figure 13. Reorientation around the molecular long axis measured in the high frequency regime. Temperature dependence T of the dielectric increment ($\square$, $\Delta\varepsilon$) and the relaxation frequency ($\bigcirc$, f_R) for compounds (*a*) 12Me and (*b*) 11Et (cooling from the isotropic phase).

for thermally activated processes, this mode slows down following an Arrhenius law in the isotropic phase, accompanied by a moderate increase of the dielectric increment. Both $\Delta\varepsilon(T)$ and $f_R(T)$ curves show a continuous behaviour in the vicinity of the isotropic to SmA and SmA to SmB phase transitions. In contrast to the behaviour of the reorientation around a molecular short axis (figure 10), the reorientation around the molecular long axis is much less affected at these phase transitions.

Further cooling into the CrE phase is accompanied by a large decrease of the dielectric increment which, however, increases again after a minimum has been

passed. Within this cooling cycle in the CrE phase, the corresponding relaxation frequency decreases slightly, but increases on further cooling until a maximum is reached at 135°C, where the relaxation frequency compares with that for the isotropic phase near the isotropic to SmA phase transition. The relaxation frequency decreases again on continuation of the cooling process. The reorientation around the molecular long axis is frozen in compound 12Me in the crystalline phase that is formed by the supercooled CrE phase.

Obviously, the temperature dependence of the reorientation around the molecular long axis of compound 12Me does not obey an Arrhenius law in the CrE phase. The slowing down of this mode, observed 10 K below the SmB to CrE phase transition, indicates that the corresponding potential describing the reorientation around the molecular long axis becomes weak. Interestingly, the activation energy of a reorientation around the molecular short axis also changes at this temperature as can be seen from figures 10 and 11. Therefore, a change of the potential acting on reorientations around the molecular long axis affects the mechanism of a reorientation around a molecular short axis. By virtue of the change of this potential, the molecules in the biaxial CrE phase might tend to move the short axes around which reorientations occur, a process which might be accompanied by a change of the activation energy related to a reorientation around the molecular short axis (figure 12).

3.3.2. *Compound 11Et*

For compound 11Et, the temperature dependence of the relaxation observed in the high frequency regime is depicted in figure 13(*b*). In the isotropic and SmA phases the behaviour resembles that of its isomer 12Me, but at the SmA to SmB phase transition, the relaxation frequency increases by at least two orders of magnitude, almost exceeding the upper range of the HF reflectometer in the SmB phase. On further cooling, this mode slows down and obeys an Arrhenius law in the CrE phase. However, at the SmB to CrE phase transition, the relaxation frequency decreases discontinuously, as well as in the vicinity of the crystallization of the CrE phase. In the crystalline phase of 11Et this mode is still active and compares to the one in the isotropic phase. This fact identifies the crystalline phase of 11Et as a disordered crystal, and 35 K below the crystallization temperature the dielectric increment decreases and the mode is frozen in.

In the isotropic and SmA phases of both isomers the relaxation frequency and the dielectric increment of the relaxation observed in the high frequency regime are very similar and this relaxation obeys the Arrhenius law with an activation energy of $14 \, \text{kJ} \, \text{mol}^{-1}$ for both

isomers. Therefore, we assign this mode to the overall reorientation around the molecular long axis, which might be at least partially locked out below the SmA to SmB phase transition of compound 11Et. A relaxation related to an intramolecular reorientation of a polar function, e.g. the $COOCH_2CH_3$ group, might enter the dielectric spectrum from the high frequency side explaining the jump of the relaxation frequency observed at the SmA to SmB phase transition of compound 11Et. This intramolecular reorientation slows down on further cooling, obeying an Arrhenius law with an activation energy between 20 and $50 \, \text{kJ} \, \text{mol}^{-1}$ decreasing from the SmB to the crystalline phase (cf. figure 14). Due to the different mechanisms assigned to the relaxation observed in the high frequency regime in the SmB, CrE, and crystalline phases of both isomers, no 'generalized' Arrhenius equation is found in any of these phases, in contrast to the behaviour of the reorientation around a molecular short axis (cf. figures 10).

4. Summary and conclusion

The mesomorphic properties of two non-chiral stilbene isomers possessing an almost equal aspect ratio of molecular shape in their most extended all-*trans*-conformation have been characterized by DSC, small angle X-ray diffraction and polarizing microscopy. Molecular reorientation around the molecular long axis and a short axis has been observed in their isotropic phases, their smectic A, hexatic smectic B, and higher ordered E phases, as well as in their crystalline phases by broad band dielectric spectroscopy.
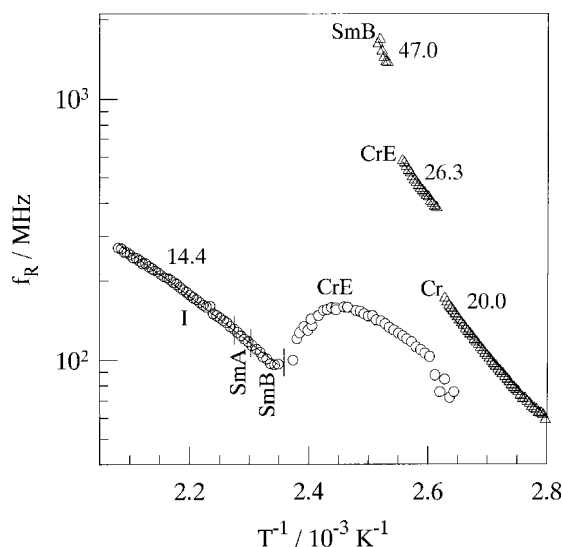

Figure 14. Logarithmic plot of the relaxation frequency f_R of the Debye mode assigned to a reorientation around the molecular long axis versus the reciprocal temperature $1/T$ for compounds 11Et ($\triangle$) and 12Me ($\bigcirc$). The numbers in the plot represent the activation energies $E_A/\text{kJ} \, \text{mol}^{-1}$.

In general, an activation energy between 71 and 78 kJ mol^{-1} characterizes the reorientation of the molecules around a molecular short axis, a process which slows down by approximately one order of magnitude at each first order phase transition between the different phases. For both compounds, one 'generalized' Arrhenius equation describes the temperature dependence of the relaxation frequency of the reorientation around a molecular short axis in each liquid crystalline phase. Therefore, the mechanism underlying this reorientation has to be very similar in the different compounds.

In contrast, the reorientation around the molecular long axis is active in the isotropic and various smectic phases in compound 12Me, but it might be locked out below the SmA to SmB phase transition of compound 11Et; an intramolecular reorientation of a polar group, which is also active in the crystalline phase of this compound, might occur instead. Within the CrE phase of compound 12Me, the mechanism related to the reorientation around a molecular short axis changes, as can be concluded from the decrease of its activation energy with decreasing temperature. This change is accompanied by a slowing down of the reorientation around the molecular long axis providing evidence for a coupling of both reorientations in the CrE phase of compound 12Me. This may be caused by a continuous movement of the molecular short axis around which the molecules reorient. This result underlines the effect of the biaxiality in the CrE phase on the molecular dynamics.

References

[1] DE GENNES, P. G., and PROST, J., 1993, *The Physics of Liquid Crystals* (Oxford: Clarendon Press).

[2] MERMIN, N. D., 1968, *Phys. Rev.*, **176**, 250.

[3] BIRGENEAU, R. J., and LITSTER, J. D., 1978, *J. Phys. (Paris) Lett.*, **39**, L399.

[4] BROCK, J. D., NOH, D. Y., MCCLAIN, B. R., LITSTER, J. D., BIRGENEAU, R. J., AHARONY, A., HORN, P. M., and LIANG, J. C., 1989, *Z. Phys. B—Condens. Matter*, **74**, 197.

[5] LANDAU, L. D., 1937, *Phys. Z. Sowjet.*, **11**, 26; [1937, *Zh. éksp. teor. Fiz.*, **7**, 19].

[6] LANDAU, L. D., 1937, *Phys. Z. Sowjet.*, **11**, 545; [1937, *Zh. éksp. teor. Fiz.*, **7**, 627].

[7] STEGEMEYER, H., 1994, *Topics in Physical Chemistry*, edited by H. Baumgärtel, E. U. Franck, and W. Grünbein, Vol. 3, *Liquid Crystals*, (Darmstadt: Steinkopff-Verlag).

[8] DOUCET, J., KELLER, P., LEVELUT, A. M., and PORQUET, P., 1978, *J. Phys. (Fr.)*, **39**, 548.

[9] LEADBETTER, A. J., GAUGHAN, J. P., KELLY, B., GRAY, G. W., and GOODBY, J. W., 1979, *J. Phys. (Fr.) Colloq.*, **40**, C3–178.

[10] GANE, P. A. C., LEADBETTER, A. J., and WRIGHTON, P. G., 1981, *Mol. Cryst. liq. Cryst.*, **66**, 247.

[11] HANDSCHY, M. A., and CLARK, N. A., 1982, *Appl. Phys. Lett.*, **41**, 1.

[12] PIERANSKI, P., GUYON, E., KELLER, P., LIÉBERT, L., KUCZYNSKI, W., and PIERANSKI, P., 1977, *Mol. Cryst. liq. Cryst.*, **38**, 275.

[13] GOUDA, F., SKARP, K., and LAGERWALL, S. T., 1991, *Ferroelectrics*, **113**, 165.

[14] SCHÖNFELD, A., and KREMER, F., 1993, *Ber. Bunsenges. phys. Chem.*, **97**, 1237.

[15] DONG, R. Y., 1987, *Bull. magn. Reson.*, **9**, 29.

[16] DOANE, J. W., 1985, *Nuclear Magnetic Resonance of Liquid Crystals*, edited by J. W. Emsley (Dordrecht: Reidel).

[17] YOUNG, C., PINDAK, R., CLARK, N. A., and MEYER, R. B., 1978, *Phys. Rev. Lett.*, **40**, 773.

[18] BATA, L., PEPY, G., and ROSTA, L., 1988, *Liq. Cryst.*, **6**, 893.

[19] BLINC, R., DOLINSEK, J., LUZAR, M., and SELIGER, J., 1988, *Liq. Cryst.*, **3**, 663.

[20] KIRST, U., and KREMER, F., 1995, *Dielektrische Spektroskopie (Spektroskopie amorpher und kristalliner Festkörper)*, edited by D. Haarer and H. W. Spieß (Darmstadt: Steinkopff-Verlag).

[21] SHEN, X., and DONG, R. Y., 1994, *Mol. Phys.*, **83**, 1117.

[22] KRESSE, H., 1983, *Adv. Liq. Cryst.*, **6**, 109.

[23] DUNMUR, D. A., FARNAN, S. P., and MURRAY, C. I., 1995, *Liq. Cryst.*, **19**, 779.

[24] BAHADUR, B., SARNA, R. K., and BHIDE, V. G., 1982, *Mol. Cryst. liq. Cryst.*, **88**, 151.

[25] BENGUIGUI, L., 1983, *Phys. Rev. A*, **28**, 1852.

[26] BUKA, A., BATA, L., and PINTER, K., 1984, *Mol. Cryst. liq. Cryst.*, **108**, 211.

[27] KRESSE, H., and GAJEWSKA, B., 1983, *Cryst. Res. Technol.*, **18**, 281.

[28] NAGABHUSHAN, C., NAIR, G. G., RATNA, B. R., SHASHIDHAR, R., and GOODBY, J. W., 1988, *Liq. Cryst.*, **3**, 175.

[29] GAJEWSKA, B., KRESSE, H., and WEISSFLOG, W., 1982, *Cryst. Res. Technol.*, **17**, 897.

[30] KRESSE, H., and BUKA, A., 1982, *Cryst. Res. Technol.*, **17**, 1123.

[31] GOUDA, F., LAGERWALL, S. T., SKARP, K., STEBLER, B., KREMER, F., and VALLERIEN, S. U., 1994, *Liq. Cryst.*, **17**, 367.